AIP | Applied Physics Letters

Real time characterization of polymer surface modifications by an atmospheric-pressure plasma jet: Electrically coupled versus remote mode

A. J. Knoll, P. Luan, E. A. J. Bartis, C. Hart, Y. Raitses, and G. S. Oehrlein

Citation: Applied Physics Letters **105**, 171601 (2014); doi: 10.1063/1.4900551
View online: http://dx.doi.org/10.1063/1.4900551
View Table of Contents: http://scitation.aip.org/content/aip/journal/apl/105/17?ver=pdfcov
Published by the AIP Publishing

Real time characterization of polymer surface modifications by an atmospheric-pressure plasma jet: Electrically coupled versus remote mode

A. J. Knoll,[1] P. Luan,[1] E. A. J. Bartis,[1] C. Hart,[1] Y. Raitses,[2] and G. S. Oehrlein[1,a)]
[1]*Department of Materials Science and Engineering and the Institute for Research in Electronics and Applied Materials, University of Maryland, College Park, Maryland 20742, USA*
[2]*Princeton Plasma Physics Laboratory, Princeton, New Jersey 08540, USA*

(Received 23 August 2014; accepted 16 October 2014; published online 27 October 2014)

We characterize and distinguish two regimes of atmospheric pressure plasma (APP) polymer interactions depending on whether the electrical interaction of the plasma plume with the surface is significant (*coupled*) or not (*remote*). When the plasma is *coupled* to the surface, localized energy deposition by charged species in filaments dominates the interactions with the surface and produces contained damaged areas with high etch rates that decrease rapidly with plasma source-to-sample distance. For *remote* APP surface treatments, when only reactive neutral species interact with the surface, we established specific surface-chemical changes and very slow etching of polymer films. Remote treatments appear uniform with etch rates that are highly sensitive to feed gas chemistry and APP source temperature. © *2014 AIP Publishing LLC*.
[http://dx.doi.org/10.1063/1.4900551]

Atmospheric-pressure plasma sources have been increasingly investigated for a wide range of applications, from biological[1–3] to industrial surface treatments.[4,5] Here, we distinguish two modes of APPJ operation depending on if the plume is coupled to the surface and charged species dominate versus remote treatments where reactive neutrals dominate. Previous work on APPJ surface interaction has not systematically distinguished between the two interaction modes described here, despite substantial difference in the physical mechanisms, and have primarily been investigated post-treatment through methods such as biological deactivation,[6] water contact angle,[7] atomic force microscopy,[8] Fourier transform infrared spectroscopy,[9] and profilometry.[10] In this work, we use a combination of *in situ* techniques including real time ellipsometry and high speed photography with post characterization techniques. We find that APP source/sample geometry, feed gas, environmental chemistry, and APP source temperature play important roles in determining the consequences of the APP-surface interactions.

The plasma source used in this work has been described previously[1] and is based on the design by Teschke *et al.* called an atmospheric-pressure plasma jet (APPJ).[11] A diagram of the experimental setup is shown in Fig. 1(a). The plasma source consists of two 20 mm long cylindrical copper electrodes separated by a 12 mm thick Teflon block around a 6.35 mm outer diameter, 3.7 mm inner diameter alumina tube through which 2 lpm Ar gas was flowed with or without 1% O_2 or N_2 admixtures. The plasma was generated using a high voltage power generator driven at 25 kHz. Applied voltage and voltage across measurement capacitor was monitored by using a Tektronix P6015A high voltage probe connected to a Hewlett-Packard 400 MHz oscilloscope. Power dissipated by the plasma was calculated using the Lissajous method using a 1 nF measurement capacitor (C_m).[12,13] High speed photography of the APPJ was taken using a Phantom v7.3 camera. An ellipsometer utilizing a 1.5 mW HeNe laser at 632.8 nm was used to non-invasively investigate thickness and index changes extracted through optical modeling of the ellipsometric data. Surface chemistry analysis by XPS was performed by a Vacuum Generators ESCALAB MK II surface analysis system post treatment. Surface morphology was imaged post treatment using a Hitachi SU-70 Analytical scanning electron microscopy (SEM) and through differential interference contrast microscopy. The surface studied was a 300 nm thick PMMA-based 193 nm photoresist polymer (PR193) film described previously.[17]

Figure 1(a) displays the two APPJ modes of operation. For the remote treatment mode, the plasma is generated with a source to nozzle distance (s_n) of 15 cm and a nozzle to sample distance (s_s) of 1 cm to ensure no direct electrical interaction. Plasma coupling mode is evident by filaments visually terminating at the film surface and occurs at combined distances closer than 15 cm, depending on gas chemistry and whether the plasma is confined within the tube (small s_n) or exposed to the ambient (small s_s). The setup also allows for the addition of a removable, electrically insulating shield between the plasma and sample (not shown).

High speed photography of the APPJ discharge with no surface interaction is shown in Fig. 1(b). The APPJ was flowed into either open air (top row) or a controlled environment matching the feed gas chemistry (middle row). Applied voltage for all gas chemistries was held constant at 14 kV peak to peak, and power dissipation was measured to be 6.2 W for Ar, 9.2 W for 1% N_2 in Ar, and 11.6 W for 1% O_2 in Ar. The pure Ar plume is concentrated in one central channel and increases in length as the environment changes from air to Ar. This central channel nature has been attributed previously to the metastable state Ar ($4^3P_2{}^0$) with 11.6 eV, which does not have enough energy to ionize Ar ($E_i = 15.8$ eV), so the plasma is only formed by streamer process.[14] N_2 addition creates a comparatively diffuse plume, with discharges branching away from the central filament and extending outward when the environment matches the feed gas. This is likely due to the introduction of Penning

a)oehrlein@umd.edu

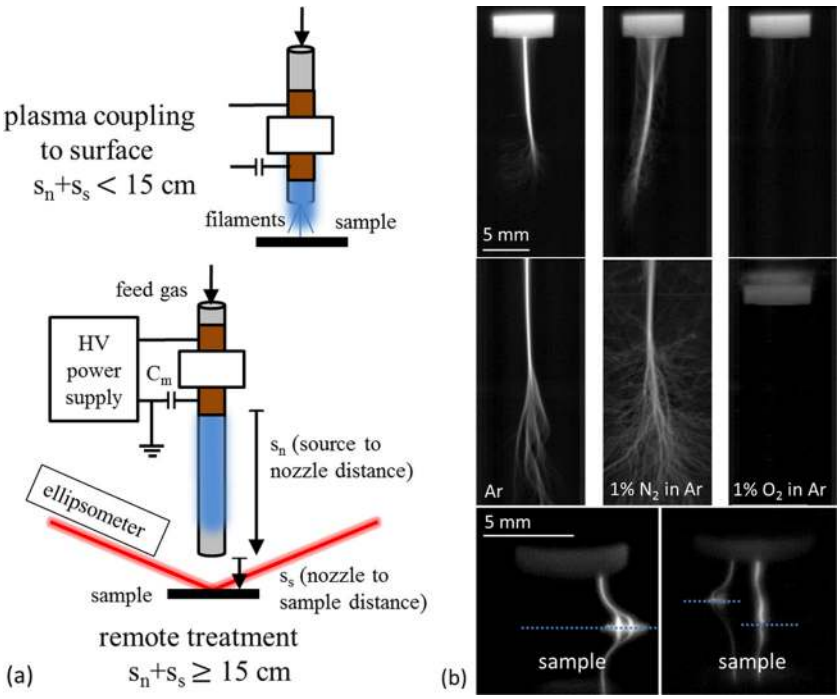

FIG. 1. (a) Experimental setup showing two distinct operational modes: remote and closely-coupled. Plasma jet can also be exposed to ambient or confined within the dielectric tube. (b) High speed photography at 100 fps, 30 ms exposure in open air (top row) and enclosed environment matching feed gas chemistry (middle row). The bottom row shows the APPJ coupling to samples, which are marked as dotted blue lines with reflections of the plasma below them.

ionization that occurs with N_2 metastable species.[15] O_2 addition to the feed gas, regardless of environment, greatly reduces the plume length and intensity. This observation suggests reduced plasma density for the addition of O_2, likely resulting from the loss of electrons by creation of negative oxygen ions[16] and is predicted by modeling O_2 addition to Ar plasma.[17] The confined geometry of the APPJ controls the gaseous environment around the plasma similar to the controlled environment shown here.

Figure 1(b) (bottom row) shows high speed photography with 30 μs exposure time of the plasma coupling to the surface. Images show filaments that extend outward from the source tube, sometimes several in one image. At close distances, the etch region is annular following the path of these filaments, as shown in Fig. 2(a). However, as the source is moved away from the sample, the diameter of the etched area shrinks from ~7 mm to 3.7 mm, matching the tube inner diameter. This agrees with previous work that shows that plasma bullet emission occurs in a ring shape.[18] Typical etch rates are locally >100 nm/min where the filaments terminate at the surface for coupled interactions compared to the remote interaction, where etch rates are below 3 nm/min. The thickness removal is lower than similar treatments by Fricke *et al.*,[10] who see etch rates above 1000 nm/min at distances of 5 mm from the sample, likely due to differences in the APPJ design.

The electrically coupled surface interaction mode visibly damages the photoresist in the form of spots due to intense, localized energy deposition, leading to fast film removal. Figure 2(b) shows a SEM image of a damage spot which has high roughness throughout the affected area. High speed photography was used during a 0.5 second treatment and the position of each filament impact was extracted. The position of these strikes is shown in Fig. 2(c) and compared to the position of the significant spot damage identified by microscopy. Areas with higher densities of strikes to the surface positively correlate with visible spots. This indicates that the plasma will more likely electrically couple to previously damaged spots. The small number of spots compared to the number of filament interactions with the surface suggests that either not all filaments cause damage or that it takes many strikes before a large spot is formed. The surface

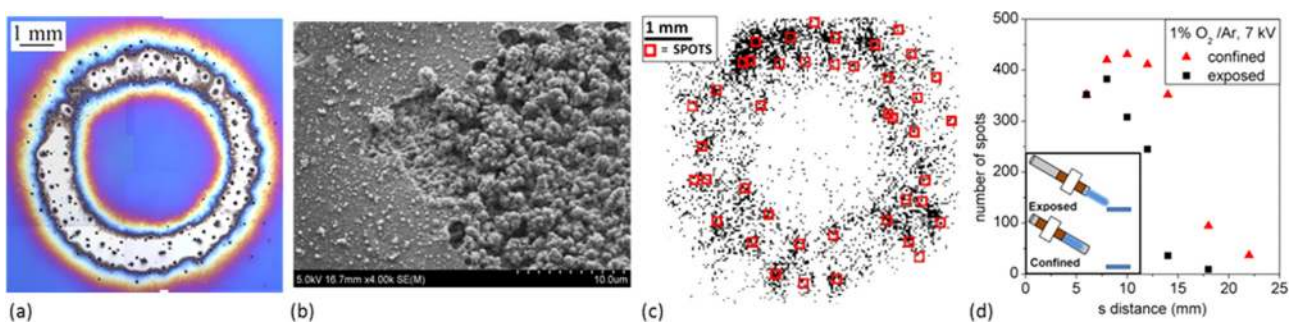

FIG. 2. (a) 1% O_2 in Ar, $s_n = 2$ mm, $s_s = 4$ mm, 30 s treatment image with interference microscopy showing annular effect. (b) SEM image showing high roughness formed at center of a spot under same conditions described in (a). (c) Graph of where filaments hit surface (black pixels) extracted from high speed photography of 0.5 s treatment compared to actual spots seen by optical microscopy (red squares). (d) Photoresist surface area etched at rates greater than 100 nm/min vs distance of source from sample ($s = s_n + s_s$) for exposed (s_n fixed at 2 mm) and confined (s_s fixed at 4 mm) conditions.

area where more than 50 nm of photoresist was removed during the 30 s treatments was determined for various source to sample distances ($s_n + s_s$) and is shown in Fig. 2(d). The amount of photoresist removed decreases as distance increases and decreases more quickly when the plasma is exposed to the ambient environment. This agrees with previous work demonstrating the importance of the ambient chemistry around the APPJ.[1] This result also agrees with the images of Fig. 1(b) which show reduced plume length in open air versus controlled environment matching feed gas, similar to how the plasma is confined in the APPJ tube.

In the following, we discuss remote plasma processing where direct electrical interaction with the sample is avoided. For pure Ar flowing into air, the etch rate of the PR193 film is initially low, called etch lag, and subsequently increases. The duration of this etch lag increases with the amount of time the plasma has been off, as shown in Fig. 3(a). We found that the increase of the polymer etching rate correlated with heating of the dielectric tube. The temperature of the APPJ source was measured by a FLIR i7 thermal imaging camera and plotted versus etch rate over several experiments to make an Arrhenius plot and estimate an apparent activation energy of ~0.9 eV. Cooling the source externally with compressed air from approximately 80 °C to 50 °C showed a reduction of 0.05 nm/min in etch rate that then increased again once cooling was stopped. This slight reduction further supports the dependence of the plasma surface interaction on source temperature.

The sample was also shielded from the APPJ (using the electrically insulating shield mentioned above), preventing etching while leaving the plasma on to prevent the dielectric tube from cooling. As shown in Fig. 3(b), etch lag does not occur and the etch rate recovers immediately after the shield is removed. This suggests that etching is not related to sample heating during the treatment since the sample would have ample time to cool while shielded. The sample temperature was estimated to increase by less than 30 °C during a 30 min argon treatment by measuring the refractive index changes of bulk Si.[19]

Feed gas chemistry at constant applied voltage plays a large role in determining plasma properties[15,20] as well as etching and surface modifications. Figures 3(c) and 3(d) show a comparison of a remote treatment with alternating pure Ar and 1% N_2 or O_2 admixture to Ar under same electrical characteristics for high speed photography work. Etch rate for N_2/Ar increases to ~2.0 nm/min, which is several times greater than for pure Ar. N_2/Ar plasma tends to extend further down the APPJ tube at similar conditions than other gas chemistries and shows increased power dissipation from pure Ar, which likely explains the increased etch rate. O_2/Ar has reduced etch rates of ~0.05 nm/min compared to pure Ar, which saturates at ~0.5 nm/min, despite having increased dissipated power. This decrease mirrors the drop in emission intensity seen in the high speed photography.

While oxygen addition to the feed gas reduces the etch rate, increased oxygen uptake at the surface is seen in XPS surface analysis (Fig. 4). The oxygenation of the surface for the pure Ar and N_2/Ar treatments likely comes from plasma interactions with ambient air. All three gas chemistries also show the formation of NO_x species at the surface. The O_2 treatment shows increased species with greater oxygen content such as NO_3, whereas the N_2 treatment shows much less NO_3 and increased species that have greater N:O ratios.

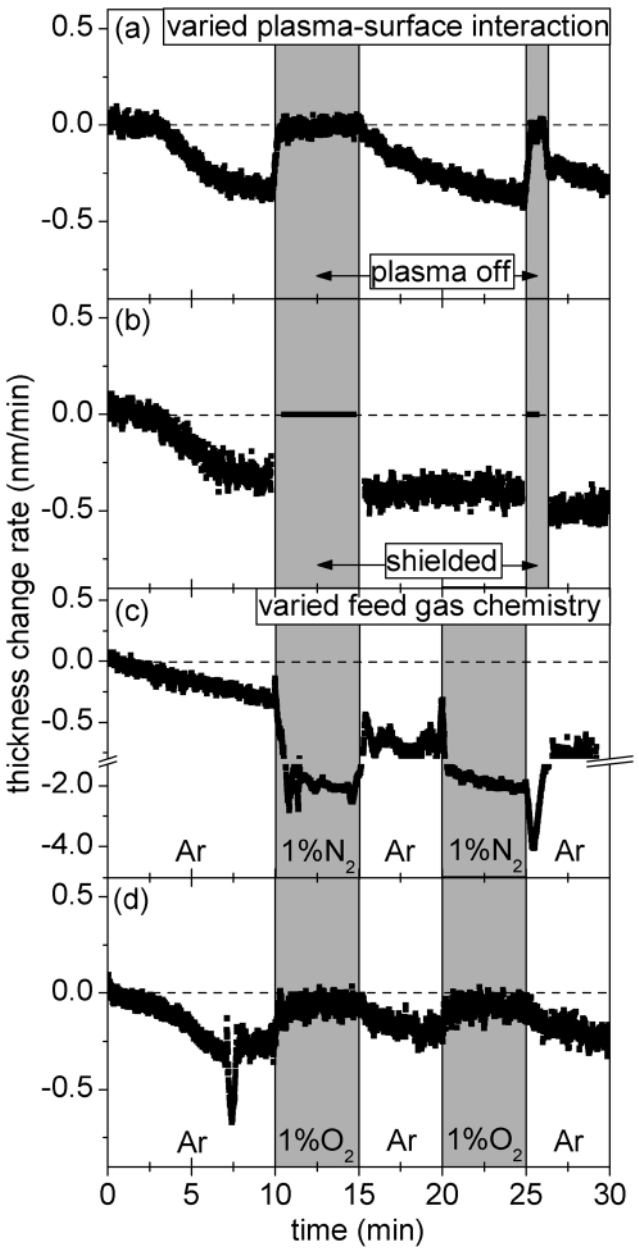

FIG. 3. Remote treatment ($s_n + s_s = 16$ cm) at 14 kV_{p-p} thickness change rate vs time for (a) cycled Ar plasma on and off, (b) cycled Ar treatment by shielding the sample from the plasma, (c) cycled Ar and Ar/N_2 treatment, and (d) cycled Ar and Ar/O_2 treatment.

In conclusion, the consequences of APP surface interactions are highly dependent on the interaction modes described here due to the distinct physics governing charged versus neutral species. Understanding what types of species dominate the interaction with the surface is critical to the operation of APP sources and control of surface functionalization. Average polymer etch rates are significantly higher when the plasma couples directly to the surface and produces localized damage as compared to the remote plasma mode interaction, which induces slow uniform etching and subtle surface chemical modifications. In the remote case, etch rate

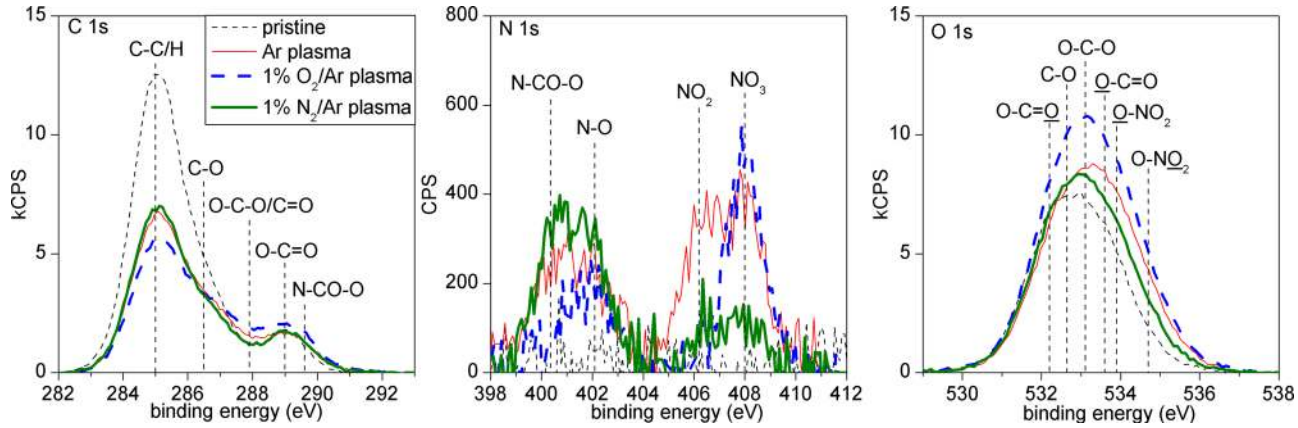

FIG. 4. XPS spectra taken after 30 min remote treatment for $(s_s + s_n) = 16$ cm comparing surface chemistry (~3 nm probing depth) of pristine PR-193 for Ar, 1% O_2/Ar, and 1% N_2/Ar treatments.

and surface modifications are highly dependent upon feed gas chemistry, APPJ source temperature, and plasma interaction with the environment.

The authors gratefully acknowledge financial support by the US Department of Energy (DE-SC0001939 and DE-SC0005105) and National Science Foundation (PHY-1004256). We also thank D. Metzler, C. Li, and E. Merino for their helpful discussion and collaboration on this project.

[1]E. A. J. Bartis, D. B. Graves, J. Seog, and G. S. Oehrlein, J. Phys. D.: Appl. Phys. **46**(31), 312002 (2013).
[2]J. Ehlbeck, U. Schnabel, M. Polak, J. Winter, T. von Woedtke, R. Brandenburg, T. von dem Hagen, and K. D. Weltmann, J. Phys. D: Appl. Phys. **44**(1). 013002 (2011).
[3]X. Pei, X. Lu, J. Liu, D. Liu, Y. Yang, K. Ostrikov, P. K. Chu, and Y. Pan, J. Phys. D: Appl. Phys. **45**(16), 165205 (2012).
[4]M. Laroussi and T. Akan, Plasma Processes Polym. **4**(9), 777 (2007).
[5]D. Pappas, J. Vac. Sci. Technol. A **29**(2), 020801 (2011).
[6]M. Y. Alkawareek, Q. T. Algwari, G. Laverty, S. P. Gorman, W. G. Graham, D. O'Connell, and B. F. Gilmore, Plos One **7**(8), e44289 (2012).
[7]C. Q. Wang and X. N. He, Surf. Coat. Technol. **201**(6), 3377 (2006).
[8]A. Sarani, A. Y. Nikiforov, N. De Geyter, R. Morent, and C. Leys, Appl. Surf. Sci. **257**(20), 8737 (2011).
[9]M. J. Pavlovich, H.-W. Chang, Y. Sakiyama, D. S. Clark, and D. B. Graves, J. Phys. D: Appl. Phys. **46**(14), 145202 (2013).
[10]K. Fricke, S. Reuter, D. Schroeder, V. Schulz-von der Gathen, K.-D. Weltmann, and T. von Woedtke, IEEE Trans. Plasma Sci. **40**(11), 2900 (2012).
[11]M. Teschke, J. Kedzierski, E. G. Finantu-Dinu, D. Korzec, and J. Engemann, IEEE Trans. Plasma Sci. **33**(2), 310 (2005).
[12]T. C. Manley, Trans. Electrochem. Soc. **84**, 83 (1943).
[13]L. A. Rosenthal and D. A. Davis, IEEE Trans. Ind. Appl. **IA-11**(3), 328 (1975).
[14]X.-J. Shao, N. Jiang, G.-J. Zhang, and Z.-X. Cao, Appl. Phys. Lett. **101**(25), 253509 (2012).
[15]R. Brandenburg, Z. Navratil, J. Jansky, P. St'ahel, D. Trunec, and H. E. Wagner, J. Phys. D: Appl. Phys. **42**(8), 085208 (2009).
[16]H. M. Katsch, C. Manthey, J. A. Wagner, and H. F. Dobele, Surf. Coat. Technol. **200**(1–4), 831 (2005).
[17]G. Park, H. Lee, G. Kim, and J. K. Lee, Plasma Processes Polym. **5**(6), 569 (2008).
[18]Y. Sakiyama, D. B. Graves, J. Jarrige, and M. Laroussi, Appl. Phys. Lett. **96**(4), 041501 (2010).
[19]G. M. W. Kroesen, G. S. Oehrlein, and T. D. Bestwick, J. Appl. Phys. **69**(5), 3390 (1991).
[20]A. Y. Nikiforov, A. Sarani, and C. Leys, Plasma Sources Sci. Technol. **20**(1), 015014 (2011).